High-pressure $Na_3(N_2)_4$, $Ca_3(N_2)_4$, $Sr_3(N_2)_4$, and $Ba(N_2)_3$ featuring nitrogen dimers with noninteger charges and anion-driven metallicity

Dominique Laniel [1,*] Bjoern Winkler,[2] Timofey Fedotenko,[1] Alena Aslandukova,[3] Andrey Aslandukov,[1] Sebastian Vogel,[4]
Thomas Meier,[3] Maxim Bykov [5] Stella Chariton,[6] Konstantin Glazyrin,[7] Victor Milman [8] Vitali Prakapenka,[6]
Wolfgang Schnick,[4] Leonid Dubrovinsky,[3] and Natalia Dubrovinskaia[1,9]

[1]*Material Physics and Technology at Extreme Conditions, Laboratory of Crystallography, University of Bayreuth, 95440 Bayreuth, Germany*
[2]*Institut für Geowissenschaften, Abteilung Kristallographie, Johann Wolfgang Goethe-Universität Frankfurt,*
Altenhöferallee 1, D-60438 Frankfurt am Main, Germany
[3]*Bayerisches Geoinstitut, University of Bayreuth, 95440 Bayreuth, Germany*
[4]*Department of Chemistry, University of Munich (LMU), Butenandtstrasse 5-13, 81377 Munich, Germany*
[5]*Department of Mathematics, Howard University, Washington, DC 20059, USA;*
The Earth and Planets Laboratory, Carnegie Institution for Science, Washington, DC 20015, USA
[6]*Center for Advanced Radiation Sources, University of Chicago, Chicago, Illinois 60637, USA*
[7]*Photon Science, Deutsches Elektronen-Synchrotron (DESY), Notkestrasse 85, 22607 Hamburg, Germany*
[8]*Dassault Systèmes BIOVIA, CB4 0WN Cambridge, United Kingdom*
[9]*Department of Physics, Chemistry and Biology (IFM), Linköping University, SE-581 83 Linköping, Sweden*

Charged molecular species, such as $[N_2]^{x-}$, $[O_2]^{x-}$, $[C_2]^{x-}$, and $[S_2]^{x-}$, follow the paradigm of carrying integer values of electrons. Here, the $Na_3(N_2)_4$, $Ca_3(N_2)_4$, $Sr_3(N_2)_4$, and $Ba(N_2)_3$ compounds were produced and characterized <70 GPa and evidenced to be composed of paradigm-breaking $[N_2]^{x-}$ dimers with noninteger charges of -0.75, -1.5, -1.5, and -0.67, respectively. The anion-driven metallicity of the compounds is proposed as the physical mechanism enabling the noninteger electron count of the $[N_2]^{x-}$ dimers. The properties of these dimers and the compounds bearing them are demonstrated to depend on their noninteger charge, paving the way to materials with electron-tunable features.

I. INTRODUCTION

Nitrogen, the main component of the atmosphere, is omnipresent. Still, the chemistry of nitrogen has long been thought to be very limited due to the extreme stability of triple-bonded molecular nitrogen. As a result, nitrogen species seemed to be constrained to the nitride (N^{3-}) and the azide (N_3^-) anions. In the last decades, tremendous efforts led to the discovery and bulk stabilization of homoatomic ions such as N_5^+ and N_5^- [1,2], providing a glimpse into the potential chemical richness of nitrogen. High-pressure investigations greatly expanded on these results, exhibiting the formation of polynitrogen species ($[N_4]^{4-}$ [3], $[N_5^-]$ [4–6], $[N_6]^{2.4-}$ [7], $[N_4]_\infty^{2-}$ [3,8,9], and N frameworks [3,10–12]).

Studies of the chemistry of nitrogen at high densities revealed the ubiquity of charged $[N_2]^{x-}$ dimers in binary nitrides [13–29]. These were discovered in the form of diazenides $[N_2]^{2-}$ in $Sr_8N_4[N_2] \cdot (e^-)_2$, $Sr_8N_4[N_2]_2$, SrN_2, and BaN_2, with N–N bond lengths (BLs) of 1.22 Å, comparable with those in protonated diazene N_2H_2 (1.21–1.25 Å) [30–32]. The family of compounds featuring charged dinitrogen species was later enlarged due to high-pressure synthesis of transition metals dinitrides (OsN_2, IrN_2, PtN_2, and TiN_2) [16,17,28] displaying tetravalent $[N_2]^{4-}$ anions with

N–N bond distances of ~ 1.4 Å, like those in hydrazine N_2H_4 (1.47 Å) [33]. The $[N_2]^{4-}$ anion is isoelectronic with the peroxide $[O_2]^{2-}$ and so was dubbed *pernitride*. Further progress in the exploration of the chemistry of nitrides brought findings of numerous compounds containing $[N_2]^{x-}$ structural units (Li_2N_2, LiN_2, FeN_2, CrN_2, RuN_2, $Re(N_2)N_2$, $Li_2Ca_3[N_2]_3$, etc.) [13,15,18,20,21,34–39] with N–N distances varying in a rather wide range (1.15–1.35 Å). For all these compounds, the formal charge (FC) of the $[N_2]^{x-}$ anion is an integer, with $x = 1$, 2, 3, or 4, with the π^* antibonding states of the nitrogen dimers partially or completely populated [40]. The paradigm of integer FCs observed in $[N_2]^{x-}$ dimers was recently questioned with the pressure synthesis of CuN_2, featuring $[N_2]^{x-}$ units with x stated to be in between 1 and 2, as well as $Na_3[N_2]_4$ [41] with $x = 0.75$ [13]. As the crystal chemistry of nitrides and their physical properties (compressibility, hardness, conductivity, optical characteristics, etc.) strongly depend on the character of $[N_2]^{x-}$ anions [21,37], further high-pressure studies of yet unexplored metal-nitrogen systems are of the utmost interest and importance.

Here, we present the results of high-pressure single-crystal x-ray diffraction (XRD) experiments in laser-heated diamond anvil cells (DACs), which reveal the binary alkali- and alkaline earth-nitrogen compounds $Na_3(N_2)_4$, $Ca_3(N_2)_4$, $Sr_3(N_2)_4$, and $Ba(N_2)_3$. The assignment of FCs to the $[N_2]^{x-}$ units in each of these compounds yields a noninteger value. We show that the FCs of the $[N_2]^{x-}$ species correlate with

_____
*Corresponding author: dominique.laniel@uni-bayreuth.de

their intramolecular BLs and the physical properties of the compounds bearing them. The mechanism enabling this remarkable phenomenon is explored through *ab initio* calculations and linked to the anion-driven metallicity of these compounds.

II. EXPERIMENTAL AND COMPUTATIONAL METHODS

A. Sample preparation

Diamond anvils with a culet diameter of 250 μm were mounted and aligned in a BX90-type screw DAC [42]. A rhenium gasket with an initial thickness of 200 μm was indented down to 25 μm, and a sample cavity of 120 μm in diameter was laser-drilled at the center of the indentation. A ruby microsphere was positioned on the diamond anvils and its calibrated fluorescence employed as a pressure gauge [43]. The DAC was then loaded with either NaN_3, $Ca(N_2)_3$, $Sr(N_2)_3$, or $Ba(N_2)_3$ as well as molecular nitrogen gas ($\sim$1200 bars) in a high-pressure vessel. NaN_3 was purchased from Sigma Aldrich ($\geqslant$99.5% purity).

$Ca(N_3)_2$ was prepared starting from NH_4N_3 and $Ca(OH)_2$ according to a literature protocol by Müller [44]. $Ca(OH)_2$ and excess of NH_4N_3 were dissolved in deionized water, and the solution was filtered to remove $CaCO_3$ residues. Water was removed from the filtrate by a rotary evaporator to yield $Ca(N_3)_2$. The obtained material was further purified by recrystallization from acetone and then dried in vacuum. NH_4N_3 was obtained according to Frierson *et al.* [45] via a 12 h sublimation (200°C → 25°C) in a Schlenk tube (open valve), starting from stoichiometric amounts of NH_4NO_3 and NaN_3.

$Sr(N_3)_2$ and $Ba(N_3)_2$ were prepared from $SrCO_3$ and dilute HN_3 [<3%, prepared from a NaN_3 solution and an ion exchanger (Amberlyst® 15, Sigma Aldrich)] according to modified protocols by Suhrmann and Clusius [46] and Karau [47]. The azides were precipitated from a concentrated aqueous solution with acetone, filtered, and dried in vacuum.

Alkaline earth azides are sensitive to moisture and light and therefore should be stored in small quantities under inert gas and the exclusion of moisture. Since HN_3 and azides are explosive and poisonous, special care is needed during preparation and handling.

B. XRD

The XRD studies were performed at the GSECARS ($\lambda = 0.2952$ Å) and P02.2 beamlines ($\lambda = 0.2891$ Å) at the Advance Photon Source (APS) and PETRA III, respectively. The structures of all reported compounds were solved and refined using single-crystal XRD analysis. Le Bail fits based on powder XRD were only used to be sure that we identified all phases, and the sample did not contain any unidentified phases—not for obtaining any structural information. To determine the sample position on which the single-crystal XRD acquisition is obtained, a full XRD mapping of the experimental chamber was performed. The sample position displaying the most single crystal reflections belonging to the phase of interest was chosen for the collection, in step scans of 0.5° from −38° to +38°, of the single-crystal XRD data. The CRYSALIS PRO software [48] was utilized for the single-crystal data analysis. The analysis procedure includes the peak search,

the removal of the parasitic reflections of the diamond anvils, finding reflections belonging to a unique single crystal, the unit cell determination, and the data integration. The crystal structures were then solved and refined within the JANA2006 software [49]. The procedure for single-crystal XRD data acquisition and analysis was previously demonstrated and successfully employed [3,12,50,51]. The full details of the methods can be found elsewhere [52]. Powder XRD was also performed to verify the chemical homogeneity of the sample. The powder x-ray data were integrated with DIOPTAS [53] and analyzed with the XRDA software [54]. Le Bail refinements (Figs. S12–S14 in the Supplemental Material [55]) employing a powder XRD pattern were accomplished with the FULLPROF software [56].

C. Raman spectroscopy

Confocal Raman spectroscopy measurements were performed with a LabRam spectrometer equipped with a ×50 Olympus objective. Sample excitation was accomplished using a continuous He-Ne laser (632.8 nm line) with a focused laser spot of $\sim$2 μm in diameter. The Stokes Raman signal was collected in a backscattering geometry by a charge-coupled device coupled to an 18001/mm grating, allowing a spectral resolution of $\sim$2 cm^{-1}. A laser power of $\sim$4.6 mW incident on the DAC was employed.

D. Laser-heating

The double-sided sample laser-heating was performed at our home laboratory at the Bayreuth Geoinstitut [57] as well as at the P02.2 [58] and GSECARS [59] beamlines of the PETRA III and APS synchrotrons, respectively, using two YAG lasers. All samples readily absorbed the YAG laser, and temperatures were accurately measured through the produced thermoemission [57]. For all samples, temperatures between 2000 and 2500 K were reached to induce a chemical reaction.

E. Computational details

First-principles calculations were carried out within the framework of density functional theory (DFT) [60] and the pseudopotential method using the CASTEP simulation package [61]. Ultrasoft pseudopotentials were generated on the fly using the parameters provided with the CASTEP distribution. These pseudopotentials have been tested extensively for accuracy and transferability [62]. The pseudopotentials were employed in conjunction with plane waves up to a kinetic energy cutoff of 570 eV. The calculations were carried out with the PBE exchange-correlation functional [63]. Monkhorst-Pack [64] grids were used for Brillouin zone integrations with a distance of <0.025 Å^{-1} between grid points. Convergence criteria included an energy change of $<5\times10^{-6}$ eV/atom for self-consistent field cycles, a maximal force of < 0.008 eV/Å, and a maximal deviation of the stress tensor <0.02 GPa from the imposed stress tensor.

III. RESULTS AND DISCUSSION

Sodium, calcium, strontium, and barium azides were each loaded into a BX90 DAC [42] along with molecular nitrogen, acting both as a reagent and a pressure transmitting

TABLE I. Selected structural parameters of the metal-nitrogen *tI*44 and *cI*112 compounds obtained from single-crystal XRD. The full crystallographic details can be found in Tables S1–S4 in the Supplemental Material [55]. The crystallographic data has been submitted under the deposition number CSD 2080210–2080213.

	Na$_3$(N$_2$)$_4$ [41]	K$_3$(N$_2$)$_4$ [65]	Ca$_3$(N$_2$)$_4$	Sr$_3$(N$_2$)$_4$	Ba(N$_2$)$_3$
Pearson symbol	*tI*44	*tI*44	*tI*44	*tI*44	*cI*112
Space group	*I*4$_1$/*amd*	*I*4$_1$/*amd*	*I*4$_1$/*amd*	*I*4$_1$/*amd*	*I*-43*d*
Pressure (GPa)	28	27	53	47	65
a(Å)	4.9597(16)	5.331(2)	4.864(2)	5.0747(11)	9.983(2)
c(Å)	16.29(7)	17.552(6)	15.758(6)	16.343(4)	9.983(2)
V(Å^3)	400.7(18)	498.8(5)	372.8(3)	420.88(17)	994.8(3)
Exp. d(N−N) (Å)	1.147(3)	1.151(11)	1.191(7)	1.19(4)	1.111(14)
	1.149(3)	1.151(10)	1.194(6)	1.20(4)	
Calc. d(N−N) (Å)	1.14	1.14	1.19	1.18	1.14
(60 GPa)	1.14	1.14	1.19	1.19	
Calc. d(N−N) (Å)	1.15	1.15	1.20	1.20	1.15
(1 bar)	1.16	1.16	1.22	1.22	
FC of [N$_2$]$^{x-}$, x	0.75	0.75	1.5	1.5	0.67

medium. Double-sided YAG laser-heating of the compressed samples was performed at various pressures between 40 and 70 GPa. The samples were then characterized by single-crystal XRD, and their structures were solved [52]. The Na$_3$(N$_2$)$_4$, Ca$_3$(N$_2$)$_4$, and Sr$_3$(N$_2$)$_4$ compounds were synthesized at pressures of 41, 53, and 47 GPa, respectively, and found to be isostructural. Their structures adopt the tetragonal symmetry (space group *I*4$_1$/*amd*, #141); the lattice parameters are provided in Table I. As an example of their common structure type, which is further referred to by its Pearson symbol *tI*44, the structure of Sr$_3$(N$_2$)$_4$ is shown in Figs. 1(a)–1(d). The full crystallographic details can be found in Tables S1–S3 in the Supplemental Material [55], and the single-crystal data were deposited in the CCDC database under the identifiers CSD 2080210–2080213. This structure

type has recently been reported for K$_3$(N$_2$)$_4$ (at 27 GPa) [65] as well as Na$_3$(N$_2$)$_4$ (at 28 GPa) [41]. A noteworthy feature of all *tI*44 compounds is that two crystallographically distinct nitrogen atoms, N1 and N2, form the two dimers, N1–N1 and N2–N2, with intramolecular distances almost identical within the experimental error [41,65]. As listed in Table I, the N1–N1 [N2–N2] intramolecular distances are of 1.147(3) Å [1.149(3) Å], 1.151(11) Å [1.151(10) Å], 1.191(7) Å [1.194(6) Å], and 1.19(4) Å [1.20(4) Å] in the Na$_3$(N$_2$)$_4$, K$_3$(N$_2$)$_4$, Ca$_3$(N$_2$)$_4$, and Sr$_3$(N$_2$)$_4$ compounds at pressures 28, 27, 53, and 47 GPa, respectively. The dimers are found to be elongated compared with nitrogen molecules (N$_2$), where the N−N distance is of ~1.10 Å [66,67] in nitrogen gas or in high-pressure solid molecular nitrogen allotropes. Upon decompression, the diffraction signal from
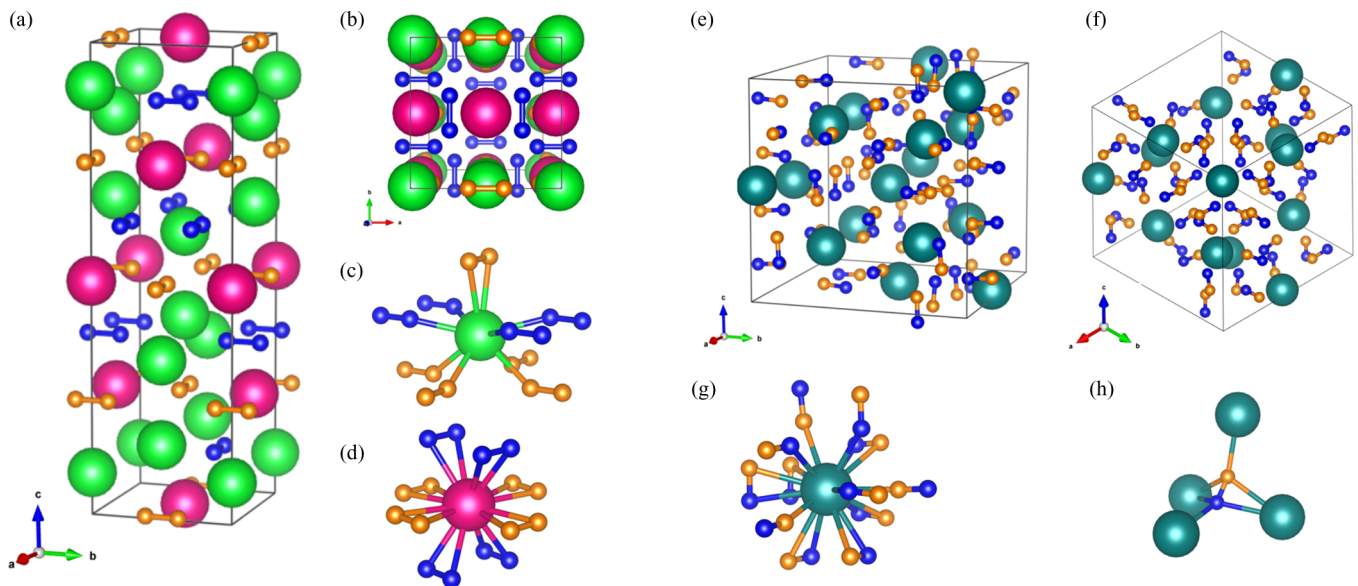
FIG. 1. Crystal structure of *tI*44 and *cI*112 compounds. (a) *tI*44 Sr$_3$(N$_2$)$_4$ at 51 GPa, (b) *tI*44 as viewed along the *c* axis, (c) Sr1 atom coordinated by nine [N$_2$] dimers, and (d) Sr2 atom coordinated by eight dimers. Color code for spheres representing different atoms: green (Sr1), pink (Sr2), blue (N1), and orange (N2). The *tI*44 Sr$_3$(N$_2$)$_4$, Ca$_3$(N$_2$)$_4$, Na$_3$(N$_2$)$_4$, and K$_3$(N$_2$)$_4$ are isostructural. (e) *cI*112 Ba(N$_2$)$_3$ at 65 GPa, (f) *cI*112 as viewed along its threefold axis, (g) Ba coordinated by 12 dimers—six side-on and six head-on, and (h) the N1-N2 dimer coordinated by four Ba atoms. The color code for spheres representing different atoms: cyan (Ba1), blue (N1), and orange (N2).

$Ca_3(N_2)_4$ and $Sr_3(N_2)_4$ could be observed down to 6 and 2 GPa, respectively. The information on the equations of state of the three *tI*44 compounds studied in this paper is provided in the Supplemental Material (Figs. S1–S3) [55].

The laser heating of $Ba(N_3)_2$ and N_2 at pressures between 51 and 69 GPa resulted in the formation of a new compound, $Ba(N_2)_3$. Its crystal structure was determined using single-crystal XRD analysis, see Tables I and S4 in the Supplemental Material [55]. The data can be accessed through the CCDC with the identifier CSD 2080210. $Ba(N_2)_3$ adopts a cubic structure (space group *I*-43*d*, #220) with the lattice parameter $a = 9.983(2)$ Å $[V = 994.8(3)$ Å$^3]$ at 65 GPa [Figs. 1(e)–1(h)]. Based on the structure solution and refinement, this structure type will be referred to by its Pearson symbol *cI*112. Only two Wyckoff positions are occupied: 16*c*, by the barium Ba1 atom, and two times 48*e*, by the two crystallographically distinct nitrogen atoms N1 and N2. As seen in Fig. 1(g), barium atoms are coordinated by 12 $[N_2]^{x-}$ dimers, six side-on and six head-on. In comparison, the cations in the *tI*44 structure have only 8 and 9 coordinating dimers. At 65 GPa, the length of N1–N2 dimers $d(N1–N2) = 1.111(14)$ Å is, within experimental error, like the length of the N_2 molecules in molecular nitrogen at the same pressure [66,67]. Each dimer has four barium first neighbors, forming a distorted tetrahedron [Fig. 1(h)]. Considering the center of mass of the $[N_2]^{x-}$ dimer rather than the two individual atoms, $Ba(N_2)_3$ is isostructural to α-Cu_3As, which is related to the A15 structure type [68]. $Ba(N_2)_3$ could be decompressed down to 12 GPa; at lower pressures, no diffraction lines characteristic of this phase could be observed. Figure S4 in the Supplemental Material [55] shows the experimental and calculated unit cell parameters and unit cell volume of the $Ba(N_2)_3$ compound with respect to pressure.

DFT calculations were performed for all three *tI*44 phases and the *cI*112 solid. The relaxed structures were found to match with the experimental models, as seen in Tables S1–S4 of the Supplemental Material [55]. The small decrease in the BL ($< 3\%$) of the calculated $N - N$ distances in the $[N_2]^{x-}$ dimers between ambient pressure and 60 GPa (Table I) highlights their incompressibility, in agreement with previous reports [37,41].

The FCs $x = 0.75, 0.75, 1.5, 1.5$, and 0.67, assigned to the $[N_2]^{x-}$ species in $Na_3(N_2)_4$, $K_3(N_2)_4$, $Ca_3(N_2)_4$, $Sr_3(N_2)_4$, and $Ba(N_2)_3$, respectively, are noninteger, contrary to what could be expected for nitrogen compounds [13,16,18,28,69] and other solids featuring homoatomic species, namely, carbon [70–72], oxygen [73–75], and sulfur dimers [76,77]. This breaks the established paradigm of integer charges discussed above. The anion charges in the *tI*44 and *cI*112 solids were determined assuming that the cations of alkali and alkaline earth metals have FCs equal to +1 and +2, respectively. At first glance, the validity of this hypothesis is not obvious, as for some subnitrides M_2N (M = Ca, Sr, Ba) the possibility of the FC of the cations to be equal to +1.5 has been discussed [30,78]. However, arguments such as short interatomic metal-metal distances in Ca_2N, Sr_2N, and Ba_2N (12 to 18% shorter than in pure metals at ambient conditions), measurements of various physical properties (resistivity, photoelectron spectroscopy, compressibility, and others), and *ab initio*
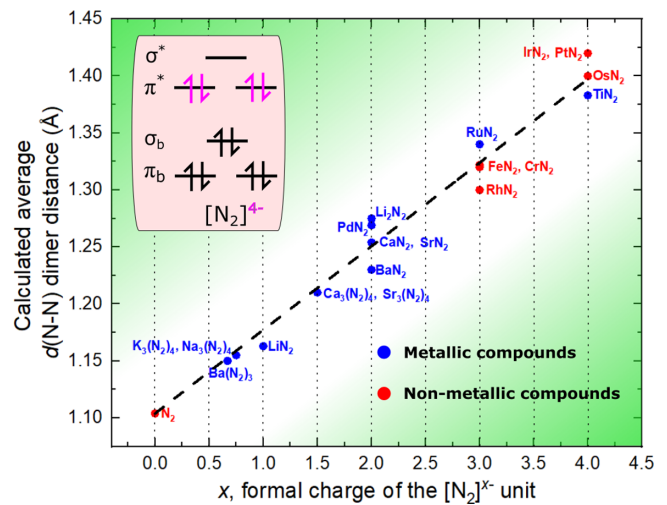
FIG. 2. Calculated (average) d(N-N) distances with respect to the formal charge (FC) x− of nitrogen dimers $[N_2]^{x-}$, for 19 simple binary compounds containing $[N_2]^{x-}$ species [13,14,22–28]. All distances were computed at 1 bar. The more complex binary compounds that contain $[N_2]^{x-}$ species along with another anionic nitrogen species were not included (e.g., Sr_4N_3 [32], ReN_2 [37]). For the FeN_2 [20], CrN_2 [35], and RhN_2 [80] compounds, the assessment of the FC of the nitrogen dimer was based on their reported Raman modes and bulk moduli. Compounds featuring $[N_2]^{x-}$ species but with missing calculated data on their intramolecular bond lengths (BLs) have been omitted. Since the charge on the $[N_2]^{x-}$ dimer in CuN_2 is not known [13], it was not included in the plot. The linear correlation between the N-N BLs and FC of the $[N_2]^{x-}$ dimers is expressed as BL = 0.074(1) Å, FC + 1.104 Å and is drawn as a dashed line. The *y* axis intercept at $x = 0$ was fixed at 1.104 Å, which is the N_2 molecule BL at 1 bar. Inset: Molecular orbital diagram of the pernitride $[N_2]^{4-}$.

calculations all advocate for subnitrides to be considered as metals described by the formula $(M^{2+})_2(N^{3-})e^-$ [78,79].

As the noninteger FCs of the $[N_2]^{x-}$ dimers in the *tI*44 and *cI*112 compounds are determined based on established crystallochemical considerations, it is more compelling to establish whether the value of *x* correlates with the geometry of the dimers and/or their chemical and physical properties. The first hint at a positive answer is that the $[N_2]^{x-}$ entities are, according to the experimental data for the *tI*44 compounds and DFT calculations for both *tI*44 and *cI*112 compounds, elongated in comparison with N_2 molecules in pure nitrogen at the same pressure [66,67]. Calculated intramolecular $[N_2]^{x-}$ BLs for numerous compounds at 1 bar are compared in Fig. 2. Considering that calculated $N - N$ intramolecular distances of 1.10 Å [66,67], 1.16–1.20 Å [13,14], 1.23–1.27 Å [14,19], 1.30–1.34 Å [25–27], and 1.38–1.42 Å [25,28] are typical for N_2, $[N_2]^-$, $[N_2]^{2-}$, $[N_2]^{3-}$, and $[N_2]^{4-}$, respectively, those found for $Na_3(N_2)_4$, $K_3(N_2)_4$, and $Ba(N_2)_3$ are intermediate to N_2 and $[N_2]^-$, while those of $Ca_3(N_2)_4$ and $Sr_3(N_2)_4$ are in between of the usual values for $[N_2]^-$ and $[N_2]^{2-}$. As seen in Fig. 2, there is a remarkable linear correlation between the $N - N$ BLs and the FCs of the $[N_2]^{x-}$ dimers. One can note that, if integer charges were assigned to dimers in the *tI*44 and *cI*122 solids, they would have shown a significant deviation from a linear dependence. Further arguments in favor of the
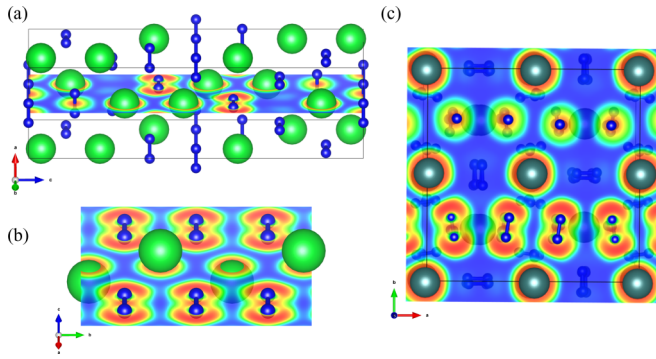
FIG. 3. Visualization of the electron localization function (ELF) analysis at 1 bar. The blue and red colors represent, respectively, no to little electron localization and a significant electron localization. The lack of pronounced electron localization in Sr$_3$(N$_2$)$_4$ between (a) Sr−Sr and Sr-[N$_2$] units [(200) slice] and (b) between [N$_2$]−[N$_2$] [(002) slice] is visible. Likewise, as shown in (c), no notable electron localization is seen in Ba(N$_2$)$_3$ [(001) slice] between any species aside from the [N$_2$]$^{x-}$ intramolecular bond. In both compounds, electron localization is never found away from an atomic site, as it would be the case for an electride.

definite correlation between the noninteger FCs of the dimers and their chemical and physical characteristics are the behavior of the N−N vibrational modes and the compressibility of the [N$_2$]$^{x-}$-bearing compounds with respect to the x value. Indeed, the comparison of the calculated phonon density of ε-N$_2$, Ba(N$_2$)$_3$, Ba$_3$(N$_2$)$_4$ (a hypothetical compound), and Ba(N$_2$) at 30 GPa in Fig. S5 in the Supplemental Material [55], as well as ε-N$_2$, Na(N$_2$)$_3$ (a hypothetical compound), Na$_3$(N$_2$)$_4$, and Na(N$_2$) also at 30 GPa in Fig. S6 in the Supplemental Material [55], demonstrates a systematic redshift of the [N$_2$]$^{x-}$ stretching mode with increasing values of x. Also, Fig. S7 in the Supplemental Material [55] shows a clear correlation between the compressibility of 15 reported binary compounds [15–17,24,80] containing [N$_2$]$^{x-}$ units and the value of $\langle d \rangle^3 / Z_{[M]} x$, where $\langle d \rangle$ is the average cation-anion distance and $Z_{[M]}$ and x are the charges on the metallic cation and on the [N$_2$]$^{x-}$ anion, respectively. Figures S8 and S9 in the Supplemental Material [55] show further correlation between

x and, respectively, the [N$_2$]$^{x-}$ dimer Mulliken charge and the [N$_2$]$^{x-}$ dimer Mulliken bond population for 12 simple binary compounds containing the [N$_2$]$^{x-}$ species.

To understand the nature of the established correlation between the [N$_2$]$^{x-}$ charge and the physicochemical properties of the tI44 and cI112 compounds, one needs to characterize the chemical bonding in these solids. Bond population analysis on all tI44 compounds and the cI112 solid (Table S5 in the Supplemental Material [55]) revealed no significant electron density between [N$_2$]–[N$_2$], M-M, and [N$_2$]-M, effectively ruling out any covalent interactions between these constituents. The electron localization function (ELF) calculations [examples for Ba(N$_2$)$_3$ and Sr$_3$(N$_2$)$_4$ are shown in Fig. 3] provide a visual corroboration. Aside from intramolecular bonding, there is no electron localization between atoms, as would have been expected for electrides. As such, in the first approximation, [N$_2$]$^{x-}$ units can be considered as isolated, and their electronic structure may be illustrated with a molecular orbital diagram, like the one shown for [N$_2$]$^{4-}$ in the inset of Fig. 2. Electrons transferred from the cations necessarily fill the π^* antibonding orbital—the lowest nonfilled energy level of the [N$_2$]$^{x-}$ species.

The most important clue to understanding these compounds is the analysis of their electron density of states (DOS), shown in Fig. 4 for Ba(N$_2$)$_3$ (and Figs. S10–S13 in the Supplemental Material [55] for the tI44 solids). It reveals that (i) all solids are metallic, agreeing well with the absence of a detected signal from Raman spectroscopy measurements made on all of them, and that (ii) essentially all the electrons in the partially filled band are contributed by the π^* orbitals of the charged [N$_2$]$^{x-}$ dimers. Indeed, the latter is verified quantitatively, where the filling of the π^* orbitals, as reflected in the partial DOS (pDOS), was computed using the following formula:

$$\frac{\int_{-\varepsilon}^{\varepsilon_{\mathrm{F}}} \mathrm{pDOS}(E)dE}{\int_{-\varepsilon}^{+\varepsilon} \mathrm{pDOS}(E)dE},$$

where $-\varepsilon$ denotes a suitably chosen energy level, ε_F is the Fermi energy, and $+\varepsilon$ is the upper energy limit. The results are shown in Table S6 in the Supplemental Material [55] and compared with the filling expected based on the FC. For example,
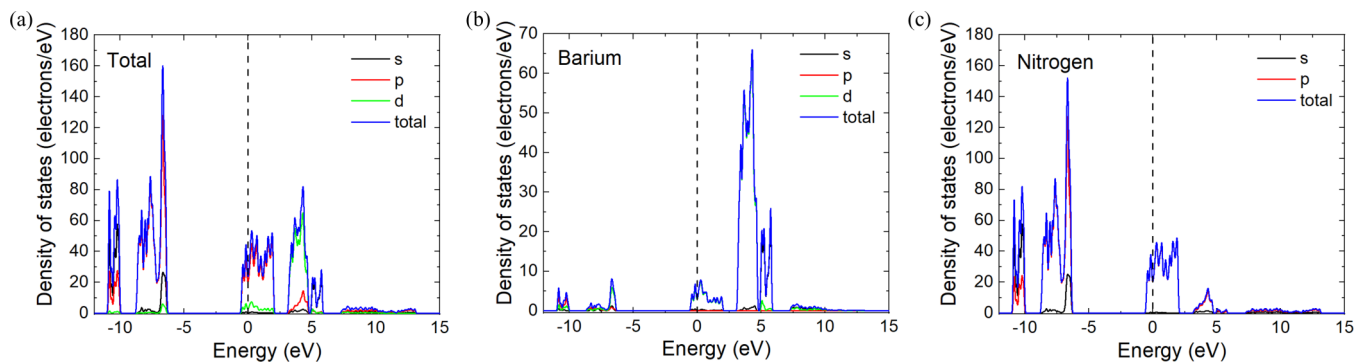
FIG. 4. Calculated electronic density of states (DOS) for the Ba(N$_2$)$_3$ compound at 1 bar. (a) The total DOS with contributions from all atoms. The compound is metallic, as seen by the nonzero DOS at the Fermi energy (set at 0 eV). (b) Partial DOS calculations, where only the electronic states belonging to nitrogen atoms were considered. The electrons constituting the partially filled band are lying on the π^* antibonding orbitals of the [N$_2$]$^{x-}$ species. (c) Partial DOS calculations, this time only showing the electronic states formed by the barium atoms. The equivalent graphs can be found for the Na$_3$(N$_2$)$_4$, K$_3$(N$_2$)$_4$, and Sr$_3$(N$_2$)$_4$ in Figs. S10–S13 in the Supplemental Material [55].

for the $Ba^{2+}[(N_2)_3]^{2-}$ compound, the FC is $-\frac{2}{3}$ for each $[N_2]$ unit, and since four electrons can be fitted into the $\pi*$ orbitals, their filling is expected to be of $(\frac{2}{3})/4 = 0.17$. For the $Ba(N_2)_3$ compound, the filling of the $\pi*$ orbitals was found to be of 0.16 based on the integrated pDOS, closely matching the 0.17 value obtained when assuming a full cation-to-anion valence electron transfer. The same remarkable agreement is observed for all four $tI44$ compounds.

The considerations described above enable us to conclude that (a) the valence electrons of the metal (Na, Ca, Sr, Ba) are almost entirely transferred to the nitrogen dimers, yielding cations (Na^+, Ca^{2+}, Sr^{2+}, Ba^{2+}) and $[N_2]^{x-}$ anions, analogously to ionic compounds; (b) the metallicity of the $tI44$ and $cI112$ solids is mainly driven by the charged $[N_2]^{x-}$ anions; and (c) the conduction electrons are effectively delocalized across the $\pi*$ orbitals of all $[N_2]^{x-}$ units, thus responsible for the exotic noninteger charge of the dinitrogen species.

The metallicity of the $tI44$ and $cI112$ is anion driven, making them different from common metals, alloys, metallic subnitrides (e.g., Ca_2N, Fig. S14 in the Supplemental Material [55]), or even metallic nitrides (e.g., NiN_2 [39], CuN_2 [13], CoN_2 [38], or TiN_2 [28]), in which the metals (e.g., Ca, Ni, Cu, Co, Ti) contribute the totality, the majority, or a significant fraction of the electrons in the conduction band. The $tI44$ and $cI112$ solids also differ from Zintl phases, among which metallic compounds are rare and explained by a heteronuclear mixing of electronic orbitals (i.e., covalent bonding), leading to a partially filled band [81,82]. The defining feature, *anion-driven metallicity*—here demonstrated to impact the geometry of the $[N_2]^{x-}$ units, phonon modes, and compressibility—makes the $tI44$ and $cI112$ solids representatives of a distinctive class of materials. Other synthetic substances, for example, polynitrogen compounds [9,10,83] and metal fullerides [84], can also be considered to belong to the class of materials with anion-driven metallicity.

IV. CONCLUSIONS

The investigation of the Na-, Ca-, Sr-, and Ba-N systems up to 70 GPa has led to the synthesis of the $Na_3(N_2)_4$, $Ca_3(N_2)_4$, $Sr_3(N_2)_4$, and $Ba(N_2)_3$ compounds. In these solids, nitrogen dimers $[N_2]^{x-}$ possess noninteger FCs x equal to -0.67, -0.75, or -1.50, thus breaking the hitherto dominating paradigm of integer-charged $[N_2]^{x-}$ dimers. The values of the charges were shown to correlate with the lengths of the dimer and the physicochemical properties of the dimer-bearing compound, thus demonstrating the fundamental importance of this parameter. The essentially complete valence electron transfer from the metal cations to the $[N_2]^{x-}$ species gives rise to anion-driven metallicity, with these electrons being delocalized on the antibonding $\pi*$ orbitals of nitrogen dimers.

In this paper, we reveal the unique nature of the $[N_2]^{x-}$ dimers and explain the origin of their noninteger FCs through insight into the electronic structure of the binary alkali- and alkaline earth metal-nitrogen compounds. These results should stimulate further analyses of the electronic structure and properties of other metallic $[N_2]^{x-}$-bearing solids. The flexibility of the $[N_2]^{x-}$ species as electron acceptors, combined with the sensitivity of their properties to the value of x, opens the way to electron-tunable materials and technologies.

[1] K. O. Christe, W. W. Wilson, J. A. Sheehy, and J. A. Boatz, Angew. Chem. Ed. **38**, 2004 (1999).

[2] C. Zhang, C. Sun, B. Hu, C. Yu, and M. Lu, Science **355**, 374 (2017).

[3] D. Laniel, B. Winkler, E. Koemets, T. Fedotenko, M. Bykov, E. Bykova, L. Dubrovinsky, and N. Dubrovinskaia, Nat. Commun. **10**, 4515 (2019).

[4] D. Laniel, G. Weck, G. Gaiffe, G. Garbarino, and P. Loubeyre, J. Phys. Chem. Lett. **9**, 1600 (2018).

[5] B. A. Steele, E. Stavrou, J. C. Crowhurst, J. M. Zaug, V. B. Prakapenka, and I. I. Oleynik, Chem. Mater. **29**, 735 (2017).

[6] M. Bykov, E. Bykova, S. Chariton, V. B. Prakapenka, I. G. Batyrev, M. F. Mahmood, and A. F. Goncharov, Dalt. Trans. **50**, 7229 (2021).

[7] N. P. Salke, K. Xia, S. Fu, Y. Zhang, E. Greenberg, V. B. Prakapenka, J. Liu, J. Sun, and J.-F. Lin, Phys. Rev. Lett. **126**, 065702 (2021).

[8] M. Bykov, E. Bykova, G. Aprilis, K. Glazyrin, E. Koemets, I. Chuvashova, I. Kupenko, C. McCammon, M. Mezouar, V. Prakapenka, H.-P. Liermann, F. Tasnádi, A. V. Ponomareva, I. A. Abrikosov, N. Dubrovinskaia, and L. Dubrovinsky, Nat. Commun. **9**, 2756 (2018).

[9] M. Bykov, E. Bykova, E. Koemets, T. Fedotenko, G. Aprilis, K. Glazyrin, H.-P. Liermann, A. V. Ponomareva, J. Tidholm, F. Tasnádi, I. A. Abrikosov, N. Dubrovinskaia, and L. Dubrovinsky, Angew. Chem. Int. Ed. **57**, 9048 (2018).

[10] M. Bykov, S. Chariton, E. Bykova, S. Khandarkhaeva, T. Fedotenko, A. V. Ponomareva, J. Tidholm, F. Tasnádi, I. A. Abrikosov, P. Sedmak, V. Prakapenka, M. Hanfland, H.

Liermann, M. Mahmood, A. F. Goncharov, N. Dubrovinskaia, and L. Dubrovinsky, Angew. Chem. Int. Ed. **59**, 10321 (2020).

[11] M. I. Eremets, A. G. Gavriliuk, I. A. Trojan, D. A. Dzivenko, and R. Boehler, Nat. Mater. **3**, 558 (2004).

[12] D. Laniel, B. Winkler, T. Fedotenko, A. Pakhomova, S. Chariton, V. Milman, V. Prakapenka, L. Dubrovinsky, and N. Dubrovinskaia, Phys. Rev. Lett. **124**, 216001 (2020).

[13] J. Binns, M.-E. Donnelly, M. Peña-Alvarez, M. Wang, E. Gregoryanz, A. Hermann, P. Dalladay-Simpson, and R. T. Howie, J. Phys. Chem. Lett. **10**, 1109 (2019).

[14] F. Peng, Y. Yao, H. Liu, and Y. Ma, J. Phys. Chem. Lett. **6**, 2363 (2015).

[15] K. Niwa, K. Suzuki, S. Muto, K. Tatsumi, K. Soda, T. Kikegawa, and M. Hasegawa, Chem. Eur. J. **20**, 13885 (2014).

[16] A. F. Young, C. Sanloup, E. Gregoryanz, S. Scandolo, R. J. Hemley, and H. K. Mao, Phys. Rev. Lett. **96**, 155501 (2006).

[17] E. Gregoryanz, C. Sanloup, M. Somayazulu, J. Badro, G. Fiquet, H. Mao, and R. J. Hemley, Nat. Mater. **3**, 294 (2004).

[18] D. Laniel, G. Weck, and P. Loubeyre, Inorg. Chem. **57**, 10685 (2018).

[19] S. B. Schneider, R. Frankovsky, and W. Schnick, Inorg. Chem. **51**, 2366 (2012).

[20] D. Laniel, A. Dewaele, and G. Garbarino, Inorg. Chem. **57**, 6245 (2018).

[21] S. B. Schneider, M. Seibald, V. L. Deringer, R. P. Stoffel, R. Frankovsky, G. M. Friederichs, H. Laqua, V. Duppel, G. Jeschke, R. Dronskowski, and W. Schnick, J. Am. Chem. Soc. **135**, 16668 (2013).

[22] Y. Shen, A. R. Oganov, G. Qian, H. Dong, Q. Zhu, and Z. Zhou, Sci. Rep. **5**, 14204 (2015).

[23] M. Wessel and R. Dronskowski, J. Comput. Chem. **31**, 1613 (2010).

[24] W. Chen, J. S. Tse, and J. Z. Jiang, J. Phys.: Condens. Matter **22**, 015404 (2010).

[25] R. Yu, Q. Zhan, and L. C. De Jonghe, Angew. Chem. Int. Ed. **46**, 1136 (2007).

[26] Z. Wang, Y. Li, H. Li, I. Harran, M. Jia, H. Wang, Y. Chen, H. Wang, and N. Wu, J. Alloys Compd. **702**, 132 (2017).

[27] Z. Zhao, K. Bao, F. Tian, D. Duan, B. Liu, and T. Cui, Phys. Rev. B **93**, 214104 (2016).

[28] V. S. Bhadram, D. Y. Kim, and T. A. Strobel, Chem. Mater. **28**, 1616 (2016).

[29] K. Niwa, T. Terabe, K. Suzuki, Y. Shirako, and M. Hasegawa, J. Appl. Phys. **119**, 065901 (2016).

[30] G. Auffermann, Y. Prots, and R. Kniep, Angew. Chem. Int. Ed. **40**, 547 (2001).

[31] V. G. Vajenine, G. Auffermann, Y. Prots, W. Schnelle, R. K. Kremer, A. Simon, and R. Kniep, Inorg. Chem. **40**, 4866 (2001).

[32] Y. Prots, G. Auffermann, M. Tovar, and R. Kniep, Angew. Chem. Int. Ed. **41**, 2288 (2002).

[33] P. A. Giguère, I. D. Liu, and D. Liu, J. Chem. Phys. **20**, 136 (1952).

[34] J. C. Crowhurst, A. F. Goncharov, B. Sadigh, J. M. Zaug, D. Aberg, Y. Meng, and V. B. Prakapenka, J. Mater. Res. **23**, 1 (2008).

[35] K. Niwa, T. Yamamoto, T. Sasaki, and M. Hasegawa, Phys. Rev. Mater. **3**, 053601 (2019).

[36] S. B. Schneider, R. Frankovsky, and W. Schnick, Angew. Chem. Int. Ed. **51**, 1873 (2012).

[37] M. Bykov, S. Chariton, H. Fei, T. Fedotenko, G. Aprilis, A. V. Ponomareva, F. Tasnádi, I. A. Abrikosov, B. Merle, P. Feldner, S. Vogel, W. Schnick, V. B. Prakapenka, E. Greenberg, M. Hanfland, A. Pakhomova, H.-P. Liermann, T. Katsura, N. Dubrovinskaia, and L. Dubrovinsky, Nat. Commun. **10**, 2994 (2019).

[38] K. Niwa, T. Terabe, D. Kato, S. Takayama, M. Kato, K. Soda, and M. Hasegawa, Inorg. Chem. **56**, 6410 (2017).

[39] K. Niwa, R. Fukui, T. Terabe, T. Kawada, D. Kato, T. Sasaki, K. Soda, and M. Hasegawa, Eur. J. Inorg. Chem. **2019**, 3753 (2019).

[40] M. Wessel and R. Dronskowski, J. Am. Chem. Soc. **132**, 2421 (2010).

[41] M. Bykov, K. R. Tasca, I. G. Batyrev, D. Smith, K. Glazyrin, S. Chariton, M. Mahmood, and A. F. Goncharov, Inorg. Chem. **59**, 14819 (2020).

[42] I. Kantor, V. Prakapenka, A. Kantor, P. Dera, A. Kurnosov, S. Sinogeikin, N. Dubrovinskaia, and L. Dubrovinsky, Rev. Sci. Instrum. **83**, 125102 (2012).

[43] A. Dewaele, P. Loubeyre, and M. Mezouar, Phys. Rev. B **70**, 094112 (2004).

[44] U. Müller, in *Berichte der Bunsengesellschaft für physikalische Chemie*, edited by D. Fair and R. F. Walker (Plenum Press, New York, 1977), Vol. 81, p. 1194.

[45] W. J. Frierson and W. F. Filbert, in *Inorganic Syntheses*, edited by W. C. Fernelius (McGraw-Hill, New York, 1946), Vol. 2, Chap. V, pp. 136–138.

[46] R. Suhrmann and K. Clusius, Z. Anorg. Allg. Chem. **152**, 52 (1926).

[47] F. Karau, High-pressure synthesis of new SrO$_2$-analogous nitrides of phosphorus as well as new processes for the preparation of metal azides, Ph.D. thesis, Ludwig-Maximilians-Universität, 2007.

[48] CRYSALIS PRO, Rigaku Corporation, https://www.rigaku.com/problealisystallography/crysalis.

[49] V. Petříček, M. Dušek, and L. Palatinus, Z. Kristallogr. Cryst. Mater. **229**, 345 (2014).

[50] D. Laniel, M. Bykov, T. Fedotenko, A. V. Ponomareva, I. A. Abrikosov, K. Glazyrin, V. Svitlyk, L. Dubrovinsky, and N. Dubrovinskaia, Inorg. Chem. **58**, 9195 (2019).

[51] D. Laniel, B. Winkler, E. Bykova, T. Fedotenko, S. Chariton, V. Milman, M. Bykov, V. Prakapenka, L. Dubrovinsky, and N. Dubrovinskaia, Phys. Rev. B **102**, 134109 (2020).

[52] E. Bykova, Single-crystal X-ray diffraction at extreme conditions in mineral physics and material sciences, Ph.D. thesis, University of Bayreuth, 2015, available online at https://epub.uni-bayreuth.de/2124/.

[53] C. Prescher and V. B. Prakapenka, High Press. Res. **35**, 223 (2015).

[54] S. Desgreniers and K. Lagarec, J. Appl. Cryst. **27**, 432 (1994).

[55] See Supplemental Material at http://link.aps.org/supplemental/10.1103/PhysRevMaterials.6.023402 for discarded alternatives for the noninteger charge of the [N$_2$]$^{x-}$ dimers; complete crystallographic data; bond population analysis; calculated filling of the π^* orbitals of the [N$_2$]$^{x-}$ dimer; pressure-volume data and equation of state; phonon density of state calculations for Ba-N and Na-N systems; compressibility of binary nitrides with [N$_2$]$^{x-}$ dimers; partial and total electronic density of states; Le Bail refinements.

[56] J. Rodríguez-Carvajal, Phys. B: Condens. Matter **192**, 55 (1993).

[57] T. Fedotenko, L. Dubrovinsky, G. Aprilis, E. Koemets, A. Snigirev, I. Snigireva, A. Barannikov, P. Ershov, F. Cova, M. Hanfland, and N. Dubrovinskaia, Rev. Sci. Instrum. **90**, 104501 (2019).

[58] H.-P. Liermann, Z. Konôpková, W. Morgenroth, K. Glazyrin, J. Bednarčik, E. E. McBride, S. Petitgirard, J. T. Delitz, M. Wendt, Y. Bican, A. Ehnes, I. Schwark, A. Rothkirch, M. Tischer, J. Heuer, H. Schulte-Schrepping, T. Kracht, and H. Franz, J. Synchrotron Radiat. **22**, 908 (2015).

[59] V. B. Prakapenka, A. Kubo, A. Kuznetsov, A. Laskin, O. Shkurikhin, P. Dera, M. L. Rivers, and S. R. Sutton, High Press. Res. **28**, 225 (2008).

[60] P. Hohenberg and W. Kohn, Phys. Rev. **136**, B864 (1964).

[61] S. J. Clark, M. D. Segall, C. J. Pickard, P. J. Hasnip, M. I. J. Probert, K. Refson, and M. C. Payne, Z. Kristallogr. Cryst. Mater. **220**, 567 (2005).

[62] K. Lejaeghere, G. Bihlmayer, T. Bjorkman, P. Blaha, S. Blugel, V. Blum, D. Caliste, I. E. Castelli, S. J. Clark, A. Dal Corso, S. de Gironcoli, T. Deutsch, J. K. Dewhurst, I. Di Marco, C. Draxl, M. Dułak, O. Eriksson, J. A. Flores-Livas, K. F. Garrity, L. Genovese *et al.*, Science **351**, aad3000 (2016).

[63] J. P. Perdew, K. Burke, and M. Ernzerhof, Phys. Rev. Lett. **77**, 3865 (1996).

[64] H. J. Monkhorst and J. D. Pack, Phys. Rev. B **13**, 5188 (1976).

[65] Y. Wang, M. Bykov, E. Bykova, X. Zhang, S. Jiang, E. Greenberg, S. Chariton, V. B. Prakapenka, and A. F. Goncharov, arXiv:2010.15995.

[66] W. Sontising and G. J. O. Beran, Phys. Rev. Mater. **4**, 063601 (2020).

[67] J. Kotakoski and K. Albe, Phys. Rev. B **77**, 144109 (2008).

[68] J. E. Iglesias and W. Nowacki, Z. Kristallogr. Cryst. Mater. **145**, 334 (1977).

[69] A. F. Young, J. A. Montoya, C. Sanloup, M. Lazzeri, E. Gregoryanz, and S. Scandolo, Phys. Rev. B **73**, 153102 (2006).

[70] M. Atoji and R. C. Medrud, J. Chem. Phys. **31**, 332 (1959).

[71] M. Atoji, J. Chem. Phys. **35**, 1950 (1961).

[72] M. Atoji, J. Chem. Phys. **46**, 1891 (1967).

[73] M. K. Y. Chan, E. L. Shirley, N. K. Karan, M. Balasubramanian, Y. Ren, J. P. Greeley, and T. T. Fister, J. Phys. Chem. Lett. **2**, 2483 (2011).

[74] H. Seyeda and M. Jansen, J. Chem. Soc. Dalt. Trans. 875 (1998).

[75] T. Bremm and M. Jansen, Z. Anorg. Allg. Chem. **610**, 64 (1992).

[76] H. Föppl, E. Busmann, and F.-K. Frorath, Z. Anorg. Allg. Chem. **314**, 12 (1962).

[77] F. Grønvold and E. Røst, Acta Cryst. **10**, 329 (1957).

[78] G. V. Vajenine, A. Grzechnik, K. Syassen, I. Loa, M. Hanfland, and A. Simon, Compt. Rendus Chim. **8**, 1897 (2005).

[79] A. Simon, Coord. Chem. Rev. **163**, 253 (1997).

[80] K. Niwa, D. Dzivenko, K. Suzuki, R. Riedel, I. Troyan, M. Eremets, and M. Hasegawa, Inorg. Chem. **53**, 697 (2014).

[81] A. V. Mudring and J. D. Corbett, J. Am. Chem. Soc. **126**, 5277 (2004).

[82] P. H. Tobash and S. Bobev, J. Solid State Chem. **180**, 1575 (2007).

[83] M. Bykov, T. Fedotenko, S. Chariton, D. Laniel, K. Glazyrin, M. Hanfland, J. S. Smith, V. B. Prakapenka, M. F. Mahmood, A. F. Goncharov, A. V. Ponomareva, F. Tasnádi, A. I. Abrikosov, T. Bin Masood, I. Hotz, A. N. Rudenko, M. I. Katsnelson, N. Dubrovinskaia, L. Dubrovinsky, and I. A. Abrikosov, Phys. Rev. Lett. **126**, 175501 (2021).

[84] K. Kamarás and G. Klupp, Dalton Trans. **43**, 7366 (2014).